Amination of a Green Solvent via Immobilized Biocatalysis for the Synthesis of Nemtabrutinib

Christopher K. Prier[1], Karla Camacho Soto[1]*, Jacob H. Forstater [1]*, Nadine Kuhl[1], Jeffrey T. Kuethe[1], Wai Ling Cheung-Lee[1], Michael J. Di Maso[1], Claire M. Eberle[1], Shane T. Grosser[1], Hsing-I Ho[1], Erik Hoyt[2], Anne Maguire[1], Kevin M. Maloney[1], Amanda Makarewicz[1], Jonathan P. McMullen[1], Jeffrey C. Moore[1], Grant S. Murphy[1], Karthik Narsimhan[1], Weilan Pan[1], Nelo R. Rivera[2], Anumita Saha-Shah[2], David A. Thaisrivongs[1], Deeptak Verma[3], Adeya Wyatt[1], and Daniel Zewge[2]

1. Process Research and Development, Merck & Co., Inc., Rahway, New Jersey 07065, United States

2. Analytical Research and Development, Merck & Co., Inc., Rahway, New Jersey 07065, United States

3. Computational and Structural Chemistry, Merck & Co., Inc., Rahway, New Jersey 07065, United States

ABSTRACT

Enzymes are capable of unique and selective transformations that can enable sustainable chemical production. While many industrial processes have been developed using free enzymes in aqueous solutions, immobilizing enzymes on a solid support can offer considerable advantages, including improved reaction efficiency, enzyme stability, the ability to perform reactions in non-aqueous media, and simplified separation of product from enzyme. Herein, we describe the development of a biocatalytic transaminase reaction of Cyrene^{TM} (**2**) utilizing an immobilized, evolved transaminase enzyme in an organic solvent to provide amine intermediate **3a** en route to the Bruton's tyrosine kinase (BTK) inhibitor nemtabrutinib. Enzyme immobilization is critical to facile isolation of the water-soluble product. Improved reaction kinetics and diastereoselectivity were achieved by bridging directed enzyme evolution with the selection of an optimal reaction solvent and solid support for immobilization, enabling a unified solvent system and direct isolation of **3a** as a crystalline salt with dr > 50:1.

Introduction

Nemtabrutinib is an investigational non-covalent Bruton's tyrosine kinase (BTK) inhibitor for the treatment of chronic lymphocytic leukemia and small lymphocytic lymphoma.[1] The molecule features the chiral cyclic amino alcohol fragment **1** (Figure 1) which was previously obtained *via* a multistep synthesis involving a number of protecting group manipulations and functional group interconversions.[2] We recently described a concise, two-step synthesis of **1** from biorenewable Cyrene[TM] **(2)**,[3] which involved an enzyme-catalyzed diastereoselective transamination of Cyrene[TM] **(2)** to form cyrene amine intermediate **3a** followed by a reductive ring opening step to yield the desired amino alcohol **1**.[4]

Transaminases catalyze a reversible conversion of ketones or aldehydes to their respective amines in the presence of a sacrificial amine donor (*i.e.* alanine, isopropylamine) and have been extensively utilized in industrial syntheses to access chiral amines.[5-10] Among commercially available transaminases, we identified that ATA-426 was uniquely effective to generate the desired *trans*-diastereomer of cyrene amine **3a** in high yield and diastereoselectivity (Figure 1).[4] ATA-426 had been previously engineered to function at elevated temperatures and pH using isopropylamine as an economical and practical amine donor.[6] While ATA-426 could provide cyrene amine **3a** with high conversion and diastereoselectivity under aqueous free-enzyme conditions (Figure 1B, Entry 1) these reactions required relatively high enzyme loading (20 wt%; see SI Tables S1 and S2). Additionally, the reaction required active pH control to avoid unproductive protonation of the amine donor and continuous acetone removal by both a headspace nitrogen sweep and vacuum to avoid increased levels of side product **4.** For example, a reaction without acetone removal resulted in significant levels of **4** (10% without vs. 2.6% with acetone removal) and suboptimal yields of **3** (75%, Figure 1B, Entry 2). While active pH control and continuous acetone removal operations were successful at laboratory scales, they presented significant challenges for reliable and robust execution at scale.
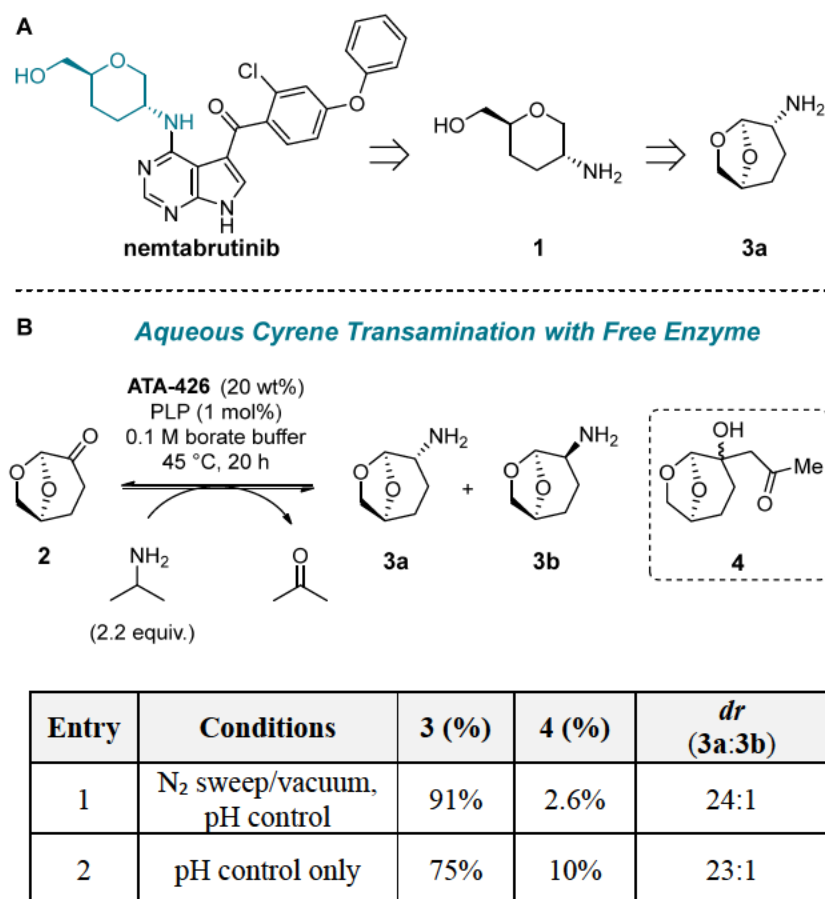
Figure 1: (A) Retrosynthesis of the amino alcohol fragment of nemtabrutinib (shown in teal) from the solvent Cyrene™ (**2**). (B) Transamination of Cyrene™ (**2**) to form cyrene amine diastereomers **3a** and **3b**, and side product **4** from an aldol reaction between acetone and **2**. Below, a tabulation of the combined assay yield of **3a** and **3b**, undesired side product **4,** and *dr*. Assay yields are determined *via* quantitative ^{1}H NMR employing an internal standard.[4]

Moreover, the aqueous transamination reaction was plagued by a cumbersome workup procedure to remove the enzyme from the highly water-soluble product **3** to allow the isolation of **3a** as a crystalline salt from an organic solvent. We envisioned that immobilization of the enzyme would address these issues, enabling enzyme operation in organic solvent and allow for facile enzyme removal from reaction streams thus simplifying product isolation.[11-15] We also hypothesized that immobilization of the transaminase enzyme could further improve the enzyme stability therefore enabling extended operation in organic solvents.[16, 17]

Herein, we describe the development of a biocatalytic transamination of Cyrene™ (**2**) in organic solvents by an evolved transaminase immobilized to a solid support. We discuss how enzyme engineering combined with immobilization and further reaction engineering were critical to develop an efficient and practical process to the desired intermediate **3a** en route to nemtabrutinib.

Results and Discussion

Enzyme immobilization

Numerous strategies for the immobilization of transaminases have been reported for both whole cells[18-20] and cell-free enzyme extracts, employing diverse immobilization modes such as covalent attachment[21-25] and non-covalent interactions[16, 26] with solid support as well as enzyme entrapment in sol-gels.[27, 28] Here, we sought to develop a cell-free, adsorption-based protocol that would use crude cell free extracts or powders to provide a robust, economical and scalable process performed in an organic solvent.

We considered different commodity macroporous resins as the enzyme solid support, as they are inexpensive and available at scales required for commercial manufacture. We prioritized resins with larger pore sizes (> 30 nm) and a high surface area to maximize protein binding *via* adsorption. Our initial tests focused on the macroporous methacrylate-based resin, HP2MGL, previously employed to immobilize transaminases in a cell-free[29, 30] and whole-cell format.[18]

The immobilizations were performed by dissolving lyophilized ATA-426 enzyme and incubating it with the resin and the pyridoxal 5′-phosphate (PLP) cofactor in potassium phosphate buffer at 4 °C as schematically depicted in Figure 2. The depletion of the enzyme from the supernatant was quantified by size exclusion chromatography (SEC) and under typical conditions the supernatant protein content decreased from ~6 wt% to 0.80 wt% over 48 hours, corresponding to an equilibrium adsorption capacity of approximately 110 mg protein/ g hydrated resin (or ~316 mg protein/g dry resin) [31]
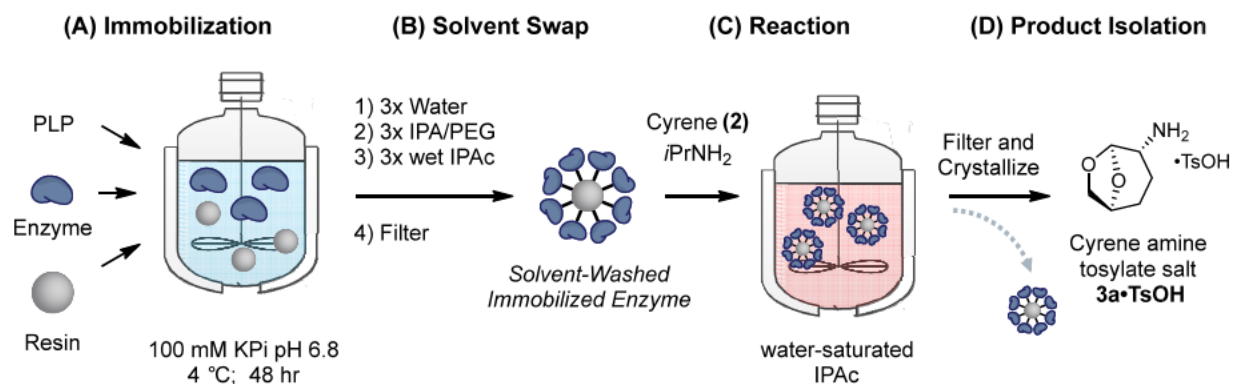

Figure 2: Schematic process for the synthesis of cyrene amine **3** using an enzyme immobilized by adsorption. **(A)** Crude cellular lysate powder containing the transaminase is dissolved in potassium phosphate buffer (KP*i*) containing PLP and mixed with the resin at 4 °C for 48 hr. **(B)** The resin is washed to remove excess PLP, unbound protein, and to displace the aqueous buffer with the desired reaction solvent. **(C)** The filtered resin is charged into a reactor containing water-saturated isopropyl acetate (IPAc), isopropylamine (*i*PrNH₂), and Cyrene™ **2** and stirred. **(D)** At the end of the reaction, the product stream is separated from the immobilized enzyme by filtration, and the cyrene amine **3a** is isolated by crystallization as the tosylate salt **3a·TsOH.**

To enable a robust amination, the biocatalytic reaction was performed in a water-saturated organic solvent.[29] To prevent the formation of a biphasic reaction mixture, it was necessary to displace the aqueous buffer used during the immobilization step with the water-saturated reaction solvent prior to adding the immobilized enzyme to the reaction vessel. To accomplish this, a series

of solvent washes were performed following the immobilization step (Figure 2B). First, unbound protein was removed using water washes which were then followed by several washes with the final water-saturated organic solvent. Such prepared resin could be filtered and charged to a reaction mixture (Figure 2, C). Utilizing this protocol, we achieved 55% conversion of 300 g/L Cyrene™ **2** to cyrene amine **3** in 24 h at 50 C using 2 equivalents of iPrNH$_2$ and 200 wt% resin, equivalent to ~11 wt% enzyme[32] relative to **2,** in water-saturated IPAc. Intriguingly, the aldol side product **4** formation was significantly decreased (5.7%) without the need for acetone removal and with only half of the enzyme loading compared to the aqueous transaminase conditions.

With this promising result in hand, we further optimized the reaction to identify the conditions that provided a suitable balance of enzyme reactivity, productivity, and side product **4** formation. Using 100 g/L Cyrene™ **2**, 1.25 equiv. iPrNH$_2$, 150 wt% resin loaded with immobilized transaminase, equivalent to 8 wt% enzyme relative to **2**, in water-saturated isopropyl acetate (IPAc) at 60 C amine **3** was produced in 80% GC area percent with a 13:1 dr after 24 h, with only 4.7% aldol by-product **4**. Amine **3a** could be isolated from the reaction stream in a facile manner by filtering the immobilized enzyme, concentrating the filtrate to remove excess iPrNH$_2$, followed by the crystallization of **3a** as the tosylate salt **3a·TsOH** from a mixture of IPAc and 2-MeTHF. Crystallization of representative streams provided both a chemical and optical purity upgrade, affording **3a·TsOH** in about 98% yield from **3** and > 20:1 dr.

While immobilization of ATA-426 on the HP2MGL resin enabled the formation of **3** in acceptable yield, the moderate dr and long reaction times offered room for improvement. To improve the performance of the immobilized transamination reaction we next opted to further engineer the transaminase enzyme with the goal to increase its activity and diastereoselectivity when immobilized.

Enzyme engineering

Using ATA-426 as a starting point for the directed evolution, the overall enzyme engineering strategy focused on iterating between: 1) identifying individual beneficial mutations via site saturation mutagenesis of the active site, surface, and core residues –based on a homology model[33] and 2) recombination of the beneficial mutations to identify improved variants (Figure 3). Given the operational complexity of high throughput enzyme immobilization, we did not perform directed evolution using immobilized variants. We hypothesized that the features limiting the enzyme under immobilization could be optimized by applying appropriate pressures in an aqueous, non-immobilized screening system. Consequently, we used temperature, solvent stability, selectivity, and substrate concentration as the evolutionary pressures to screen large mutant libraries for transamination under aqueous conditions and only the top-performing variants from each round of engineering were assayed in the immobilized format in organic solvent (see SI for experimental details).

In the first round of evolution, we targeted the residues surrounding the active site, surface and core of the protein via site saturation mutagenesis. A variant containing the A5L mutation displayed a 1.4-fold increased activity (Figure 3) and ~2-fold improved expression from high throughput lysates. Subsequent recombination of the A5L-mutant (Rd2BB) with additional beneficial mutations identified in Rd1 afforded a 2.7-fold more active variant under aqueous conditions, which was chosen as the next round backbone (Rd3BB). The third round of evolution focused on identifying mutations beneficial for selectivity. Saturation mutagenesis of the active

site residues identified an additional mutation V69A that resulted in a significantly increased selectivity (40:1 *dr*) and 1.5-fold improved catalytic activity under aqueous conditions.

In the final round of evolution, we sought to increase the enzyme thermostability and activity at elevated temperatures in organic solvents. To identify thermostabilizing mutations, selected variants from previous rounds of evolution with improved activity were subjected to a heat challenge (10 min at 70 °C) and assayed for residual activity. The screen identified thirteen stabilizing mutations which were then recombined with the mutations identified as beneficial for selectivity from Round 3. Variants generated from this combinatorial library were subjected to an increased heat challenge at 76 °C in Round 4. This library yielded the final variant termed ATA-492, which harbored five additional mutations (Figure 3). ATA-492 displayed an overall 4-fold improvement in activity, increased diastereoselectivity (88:1 *dr*) and thermostability (T_{50} = 83 °C) relative to the parent ATA-426.

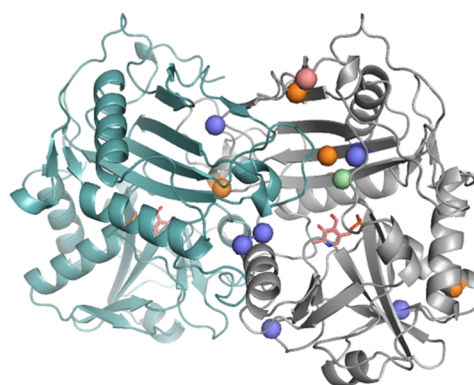| Round	Variant	Mutations relative to previous backbone	Rate (mM/min)	*dr* (*R:S*)	T_{50} (°C)
-	ATA-426	-	0.5	19:1	71.1
1	Rd2BB	A5L	0.7	20:1	71.6
2	Rd3BB	I55V;I122M;A192S; G193I;F215H;I263M	1.9	21:1	76.4
3	Rd4BB	V69A	2.8	40:1	76.4
4	ATA-492	P48V;T62A;F88W; W124G;E256R	2.1	88:1	83.2

Figure 3. Four rounds of directed evolution starting from ATA-426 provided ATA-492, an enzyme for Cyrene™ transamination with improved activity, selectivity, and thermostability. Assay conditions: 75 g/L Cyrene™ **2**, 10 wt% transaminase lyophilized lysate, 1 g/L PLP, 0.1 M sodium borate buffer pH 10.5, 1 M *i*PrNH₂, 45 °C. Rates measured by quantitative ^{1}H NMR using maleic acid as internal standard; *dr* measured after 17 h by LC after DNFB derivatization. T_{50} measured as temperature at which the enzyme retains 50% of its original activity; determined by assaying activity after the enzyme is subject to a 10 min heat challenge. Ribbon diagram shows the transaminase dimer, with PLP in pink. Mutations are represented as spheres and shown in one monomer of the enzyme dimer for clarity. DNFB = 1-fluoro-2,4-dinitrobenzene.

Reaction Solvent Optimization

Next, we compared the performance of the immobilized ATA-492 and ATA-426 in water-saturated IPAc (Figure 4A). The reactions were tested using a SpinChem rotating bed reactor (RBR), which holds the catalyst in a rotating basket suspended in the bulk liquid, allowing automated sampling from the liquid phase. In water-saturated IPAc the immobilized ATA-492 provided ~4.6-fold enhancement of the initial rate over ATA-426, with reactions proceeding to >98% cyrene amine **3** (**3a** and **3b**) after 14 h (see SI Table S4). These results demonstrated that the improvements identified with the free enzyme under aqueous conditions during the enzyme evolution translated well to the immobilized enzyme performance in an organic solvent. Interestingly, using ATA-426 the product *dr* did not exhibit significant erosion over the course of the reaction while for ATA-492 a high *dr* could be observed at early reaction stages (34:1 *dr* at

50% amine **3**) which eroded as the reaction progressed (~10:1 at >95% cyrene amine **3**, over 30 h, Figure 4A). This decrease in diastereoselectivity is consistent with the reversible mechanism of a PLP-dependent enzymatic transamination (Figure 1B).[34] We envisaged the drop in diastereomeric purity could be effectively mitigated by separating the immobilized enzyme from the reaction once the desired conversion and *dr* is achieved to provide a stable solution of **3**.
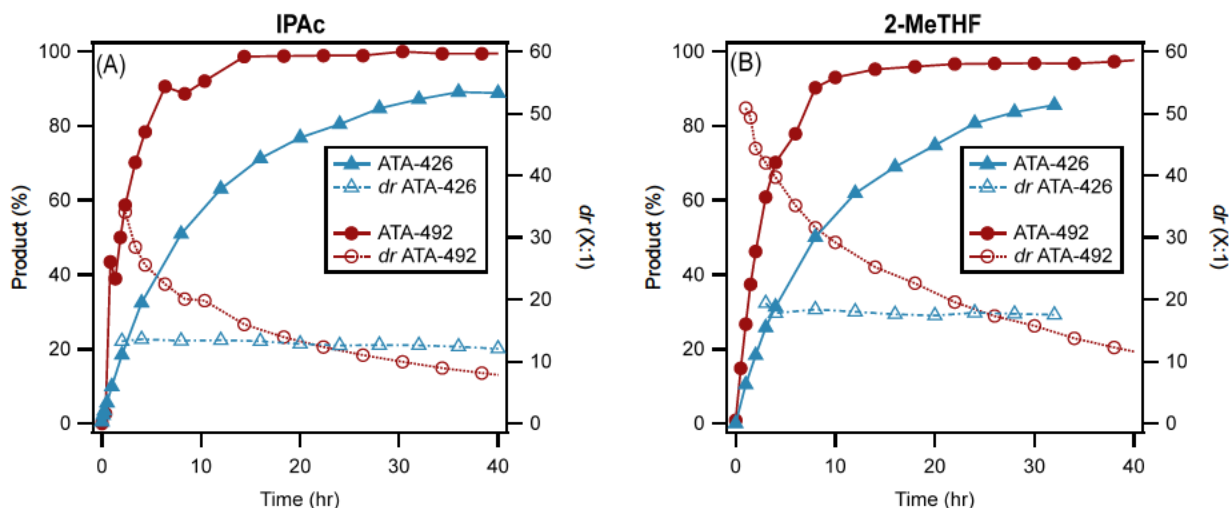

Figure 4: Kinetic profiles for transamination reactions with immobilized ATA-426 or ATA-492. GC area percent of both diastereomers **3a** and **3b** and **3a**:**3b** *dr* is recorded as a function of time **(A)** in water-saturated IPAc; **(B)** in water-saturated 2-MeTHF. Both reactions were performed at 60 C using 150 wt% resin (equivalent to 8 wt% enzyme loading relative to **2**), 100 g/L Cyrene[TM] (**2**), 1.25 equiv. *i*PrNH₂, in the indicated water-saturated solvent Connecting lines shown only as visual guide.

In addition to *dr* erosion over time, we also observed lower *dr* in the immobilized reactions in IPAc compared to the non-immobilized aqueous reactions. Solvent effects on enzyme stereoselectivity have been observed, particularly in lipase-catalyzed biotransformations.[35] This prompted us to explore additional solvents for the transamination, where we identified water-saturated 2-MeTHF as a superior reaction medium (see SI Table S5). The immobilized ATA-492 transaminase displayed higher diastereoselectivity in water-saturated 2-MeTHF compared to IPAc while retaining a similar kinetic profile (Figure 4, 32:1 *vs.* 20:1 *dr* at ~90% cyrene amine **3**). While the use of 2-MeTHF resulted in slightly elevated levels of the aldol side product **4** (for example 3.6% *vs.* 1.3%, respectively after 14 h), we selected 2-MeTHF for further studies as **4** could be effectively removed during the crystallization. Beyond the increased selectivity, the use of 2-MeTHF provided additional benefits of employing a single solvent for both the reaction and the subsequent crystallization of **3a·TsOH** as well as aligning the process around a single biorenewable solvent.

Further Resin Optimization

To further increase the reaction productivity, we evaluated a broad set of resins available at commercial scale (Fig 5). The selected resins comprised a diverse set of matrices and functional chemistries that could offer improved adsorption kinetics and/or increase the binding selectivity of the active transaminase *vs.* host cell proteins.
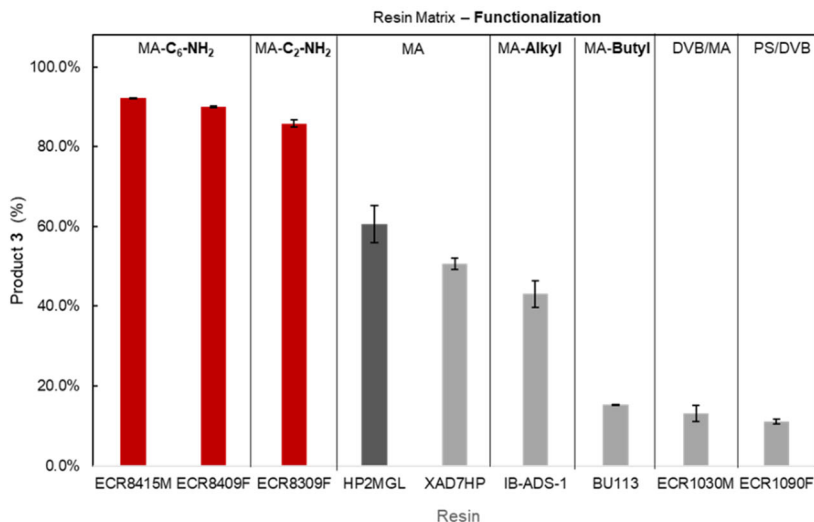
Figure 5. Resin Screen (GC area percent of both diastereomers **3a** and **3b** at 16.5 hr) for ATA-492 immobilized on resins specified. The resin matrix (MA = methacrylate, DVB = divinylbenzene, PS = polystyrene) and vendor disclosed functionalization (in bold) are listed. Reactions were performed in 2-MeTHF, as described in Figure 4. Resins functionalized with an alkylamine are colored red. HP2MGL is colored dark grey. Error bars are SEM, *n*=2.

For each resin, the immobilization of transaminase ATA-492 was conducted under identical conditions and the transamination reaction performance was determined at a fixed 16.5 hr time point. Resins with less polar surface functionalization or polymer matrices compared to HP2MGL did not show improvements in performance as did a resin with similar chemistry to HP2MGL but lower pore volume and surface areas (XAD7HP). Immobilization of the enzyme on the hydrophilic methacrylate-based resins functionalized with an alkylamine linker (ECR8309F, ECR8409F, ECR8415F), however, resulted in the highest amine product **3** ($\geq$ 86%) compared to HP2MGL resin (60.6%).

We hypothesize that under the immobilization conditions (pH 6.8), the transaminase (calculated pI 4.9 for ATA-492) and the amino-derivatized resin are oppositely charged, resulting in an increased adsorption and/or retention of the active enzyme to the alkylamine ECR resins over E. coli proteins. In contrast, the binding mode of the crosslinked methacrylate resin HP2MGL relies on hydrogen bonding and does not provide any detectable selectivity for the transaminase under the immobilization conditions.

Consistent with this hypothesis, the ATA was more selectively immobilized over *E. coli* proteins present in the crude cell lysate. We estimate an approximately 50% enrichment in ATA relative to host cell proteins based on the analysis of the change in protein composition in the supernatant by SDS-PAGE and SEC (SI Table S6, SI Fig S6). We observed further activity improvements with the immobilized ATA-492 using resins with longer amine spacers (C_2 to C_6, ECR8309F vs ECR8409F, respectively) and increased median pore size (90 nm to 150 nm,

ECR8409F vs ECR8415F, respectively). These further improvements could be attributed to a reduced enzyme crowding or mass transfer limitations.
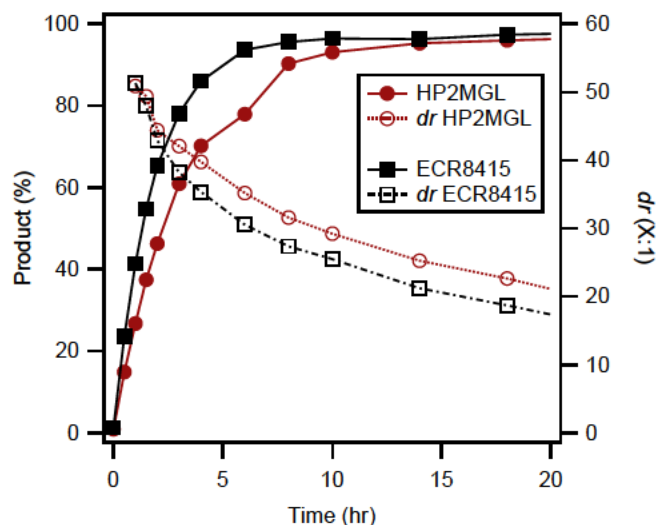

Figure 6: Transamination reaction profiles using ATA-492 immobilized on different resins (HP2MGL, red) and ECR8415F (black) in 2-MeTHF. Reactions were performed using conditions as described in Figure 4. Connecting lines shown only as visual guide.

The combined improvements achieved *via* enzyme engineering, introduction of a NH_2-C_6-linker solid support, and 2-MeTHF as the reaction solvent provided the basis for the "second generation" process to cyrene amine **3** (Figure 6). The initial reaction rate using ATA-492 immobilized on ECR8415F was 38% faster compared to the analogous reactions using the HP2MGL resin. The reaction at 10-gram scale formed **3** (**3a** and **3b**) in 91.8% yield and 22:1 *dr* in just 7 hr. Simple filtration removed the enzyme; the filtrate was concentrated and **3** was crystallized as a the tosylate salt **3a·TsOH** (see SI) in 73.2% isolated yield which upgraded the *dr* to 51:1.

With the identification of the ECR8415F resin as a more selective resin for the immobilization of ATA-492, we recognized multiple opportunities to further improve process efficiency. For example, using ECR8415F with otherwise typical immobilization conditions we were able to reduce the total immobilization time to just 4 h (*vs.* 48 h for HP2MGL) (see SI Figure S7). Additionally, we recognized the opportunity to reduce the excess enzyme utilized in the immobilization process which equals to ~ 17.5 wt% relative to **2** for a transamination reaction with 150 wt% resin as described above. Gratifyingly, by systematically decreasing the enzyme loadings in the immobilization process with ATA-492 and the ECR8415F resin, we were able to obtain a comparable reaction performance (96.5% GC area percent of amine **3**, *dr* ~ 25:1) by extending the reaction to 120 hours while utilizing only 2 wt% total enzyme relative to **2** for the entire process of immobilization and transamination (see SI Figs S8 and S9). The ability to reduce enzyme loading about 9-fold without detrimental effects to the reaction performance further showcases the combined impact of enzyme evolution and careful resin selection on the enzyme activity.

Cyrene amination with immobilized enzyme
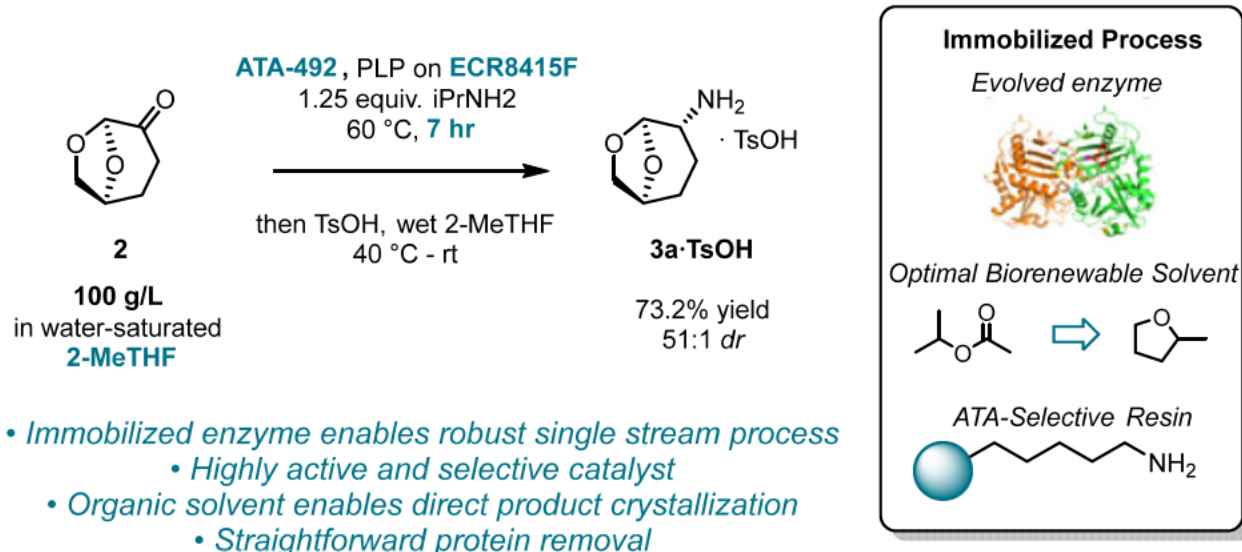
Figure 7: A combination of enzyme engineering and process optimization enables an efficient "second generation" system for the amination of Cyrene™ (**2**).

Conclusion

In conclusion, we have developed a highly efficient enzyme method to access cyrene amine intermediate **3a** en route to BTK-inhibitor nemtabrutinib. The reaction inputs are inexpensive commodity chemicals that are widely available including two biorenewable solvents (Cyrene™ (**2**) and 2-MeTHF). Through a combination of protein engineering, enzyme immobilization, and reaction optimization, we achieved a streamlined, robust process that eliminates the need for active pH control and continuous acetone removal, reduces enzyme requirements, and enables simplified, direct isolation of **3a** as a crystalline salt with dr > 50:1. The efficient and robust synthesis of chiral amines remains a critical challenge in pharmaceutical synthesis, however, as detailed in this paper, the integration of enzyme and reaction engineering methodologies offer unique opportunities to address future synthetic challenges.

ASSOCIATED CONTENT

Supporting Information. Detailed experimental and analytical methodologies, compound characterization, DNA and protein sequences of all enzymes, additional characterization and experimental.

The following files are available free of charge.
Supporting Information (pdf)

AUTHOR INFORMATION

Corresponding Authors

*Karla Camacho Soto- Email: karla.camacho.soto@merck.com
*Jacob H. Forstater- Email: jacob.forstater@merck.com

Author Contributions

The manuscript was written through contributions of all authors. All authors have given approval to the final version of the manuscript.

ACKNOWLEDGMENTS

ABBREVIATIONS

2-MeTHF- 2-Methyltetrahydrofuran

PLP- Pyridoxal 5-phosphate

IPAc- isopropyl acetate

iPrNH$_2$- isopropylamine

KPi – Potassium Phosphate

TsOH – *para*-toluenesulfonic acid

REFERENCES

(1) Reiff, S. D.; Mantel, R.; Smith, L. L.; Greene, J. T.; Muhowski, E. M.; Fabian, C. A.; Goettl, V. M.; Tran, M.; Harrington, B. K.; Rogers, K. A.; et al. The Btk Inhibitor Arq 531 Targets Ibrutinib-Resistant Cll and Richter Transformation. *Cancer Discov* **2018**, *8* (10), 1300-1315. DOI: 10.1158/2159-8290.CD-17-1409.

(2) Kriek, Nicole M. A. J.; Hout, Elise van d.; Kelly, P.; Meijgaarden, Krista E. v.; Geluk, A.; Ottenhoff, Tom H. M.; Marel, Gijs A. van d.; Overhand, M.; Boom, Jacques H. v.; Valentijn, A. Rob P. M.; et al. Synthesis of Novel Tetrahydropyran-Based Dipeptide Isosters by Overman Rearrangement of 2,3-Didehydroglycosides. *Eur. J. Org. Chem.* **2003**, *2003* (13), 2418-2427. DOI: 10.1002/ejoc.200200710.

(3) Camp, J. E. Bio-Available Solvent Cyrene: Synthesis, Derivatization, and Applications. *ChemSusChem* **2018**, *11* (18), 3048-3055. DOI: 10.1002/cssc.201801420.

(4) Kuhl, N.; Turnbull, B. W. H.; Ji, Y.; Larson, R. T.; Shevlin, M.; Prier, C. K.; Chung, C. K.; Desmond, R.; Guetschow, E.; He, C. Q.; et al. Utilizing Biocatalysis and a Sulfolane-Mediated Reductive Acetal Opening to Access Nemtabrutinib from Cyrene. *Green Chem.* **2023**, *25* (2), 606-613. DOI: 10.1039/d2gc04117k.

(5) Guo, F.; Berglund, P. Transaminase Biocatalysis: Optimization and Application. *Green Chem.* **2017**, *19* (2), 333-360. DOI: 10.1039/c6gc02328b.

(6) Yasuda, N.; Cleator, E.; Kosjek, B.; Yin, J. G.; Xiang, B. P.; Chen, F.; Kuo, S. C.; Belyk, K.; Mullens, P. R.; Goodyear, A.; et al. Practical Asymmetric Synthesis of a Calcitonin Gene-Related Peptide (Cgrp) Receptor Antagonist Ubrogepant. *Org. Process Res. Dev.* **2017**, *21* (11), 1851-1858. DOI: 10.1021/acs.oprd.7b00293.

(7) Savile, C. K.; Janey, J. M.; Mundorff, E. C.; Moore, J. C.; Tam, S.; Jarvis, W. R.; Colbeck, J. C.; Krebber, A.; Fleitz, F. J.; Brands, J.; et al. Biocatalytic Asymmetric Synthesis of Chiral Amines from Ketones Applied to Sitagliptin Manufacture. *Science* **2010**, *329* (5989), 305-309. DOI: 10.1126/science.1188934.

(8) Novick, S. J.; Dellas, N.; Garcia, R.; Ching, C.; Bautista, A.; Homan, D.; Alvizo, O.; Entwistle, D.; Kleinbeck, F.; Schlama, T.; et al. Engineering an Amine Transaminase for the Efficient Production of a Chiral Sacubitril Precursor. *ACS Catal.* **2021**, *11* (6), 3762-3770. DOI: 10.1021/acscatal.0c05450.

(9) Slabu, I.; Galman, J. L.; Lloyd, R. C.; Turner, N. J. Discovery, Engineering, and Synthetic Application of Transaminase Biocatalysts. *ACS Catal.* **2017**, *7* (12), 8263-8284. DOI: 10.1021/acscatal.7b02686.

(10) Kelly, S. A.; Pohle, S.; Wharry, S.; Mix, S.; Allen, C. C. R.; Moody, T. S.; Gilmore, B. F. Application of Omega-Transaminases in the Pharmaceutical Industry. *Chem. Rev.* **2018**, *118* (1), 349-367. DOI: 10.1021/acs.chemrev.7b00437.

(11) Boudrant, J.; Woodley, J. M.; Fernandez-Lafuente, R. Parameters Necessary to Define an Immobilized Enzyme Preparation. *Process Biochem.* **2020**, *90*, 66-80. DOI: 10.1016/j.procbio.2019.11.026.

(12) Cao, L. *Carrier-Bound Immobilized Enzymes: Principles, Application and Design*; Wiley-VCH, 2005.

(13) Sheldon, R. A.; van Pelt, S. Enzyme Immobilisation in Biocatalysis: Why, What and How. *Chem. Soc. Rev.* **2013**, *42* (15), 6223-6235. DOI: 10.1039/c3cs60075k.

(14) Thompson, M. P.; Peñafiel, I.; Cosgrove, S. C.; Turner, N. J. Biocatalysis Using Immobilized Enzymes in Continuous Flow for the Synthesis of Fine Chemicals. *Org. Process Res. Dev.* **2018**, *23* (1), 9-18. DOI: 10.1021/acs.oprd.8b00305.

(15) Romero-Fernandez, M.; Paradisi, F. Protein Immobilization Technology for Flow Biocatalysis. *Curr. Opin. Chem. Biol.* **2020**, *55*, 1-8. DOI: 10.1016/j.cbpa.2019.11.008.

(16) Bohmer, W.; Volkov, A.; Engelmark Cassimjee, K.; Mutti, F. G. Continuous Flow Bioamination of Ketones in Organic Solvents at Controlled Water Activity Using Immobilized Omega-Transaminases. *Adv Synth Catal* **2020**, *362* (9), 1858-1867. DOI: 10.1002/adsc.201901274.

(17) Stepankova, V.; Bidmanova, S.; Koudelakova, T.; Prokop, Z.; Chaloupkova, R.; Damborsky, J. Strategies for Stabilization of Enzymes in Organic Solvents. *ACS Catal.* **2013**, *3* (12), 2823-2836-2836. DOI: 10.1021/cs400684x.

(18) Andrade, L. H.; Kroutil, W.; Jamison, T. F. Continuous Flow Synthesis of Chiral Amines in Organic Solvents: Immobilization of E. Coli Cells Containing Both Omega-Transaminase and Plp. *Org. Lett.* **2014**, *16* (23), 6092-6095. DOI: 10.1021/ol502712v.

(19) Cai, B.; Wang, J.; Hu, H.; Liu, S.; Zhang, C.; Zhu, Y.; Bocola, M.; Sun, L.; Ji, Y.; Zhou, A.; et al. Transaminase Engineering and Process Development for a Whole-Cell Neat Organic Process to Produce (R)-A-Phenylethylamine. *Org. Process Res. Dev.* **2021**, *26* (7), 2004-2012. DOI: 10.1021/acs.oprd.1c00409.

(20) Rehn, G.; Grey, C.; Branneby, C.; Lindberg, L.; Adlercreutz, P. Activity and Stability of Different Immobilized Preparations of Recombinant E. Coli Cells Containing Ω-Transaminase. *Process Biochem.* **2012**, *47* (7), 1129-1134. DOI: 10.1016/j.procbio.2012.04.013.

(21) Benítez-Mateos, A. I.; Contente, M. L.; Velasco-Lozano, S.; Paradisi, F.; López-Gallego, F. Self-Sufficient Flow-Biocatalysis by Coimmobilization of Pyridoxal 5′-Phosphate and ω-Transaminases onto Porous Carriers. *ACS Sustainable Chem. Eng.* **2018**, *6* (10), 13151-13159. DOI: 10.1021/acssuschemeng.8b02672.

(22) Heckmann, C. M.; Dominguez, B.; Paradisi, F. Enantio-Complementary Continuous-Flow Synthesis of 2-Aminobutane Using Covalently Immobilized Transaminases. *ACS Sustainable Chem. Eng.* **2021**, *9* (11), 4122-4129. DOI: 10.1021/acssuschemeng.0c09075.

(23) Wang, X.; Xie, Y.; Wang, Z.; Zhang, K.; Wang, H.; Wei, D. Efficient Synthesis of (S)-1-Boc-3-Aminopiperidine in a Continuous Flow System Using Ω-Transaminase-Immobilized Amino-Ethylenediamine-Modified Epoxide Supports. *Org. Process Res. Dev.* **2022**, *26* (5), 1351-1359. DOI: 10.1021/acs.oprd.1c00217.

(24) Yi, S.-S.; Lee, C.-w.; Kim, J.; Kyung, D.; Kim, B.-G.; Lee, Y.-S. Covalent Immobilization of Ω-Transaminase from Vibrio Fluvialis Js17 on Chitosan Beads. *Process Biochem.* **2007**, *42* (5), 895-898. DOI: 10.1016/j.procbio.2007.01.008.

(25) Mallin, H.; Menyes, U.; Vorhaben, T.; Höhne, M.; Bornscheuer, U. T. Immobilization of Two (R)-Amine Transaminases on an Optimized Chitosan Support for the Enzymatic Synthesis of Optically Pure Amines. *ChemCatChem* **2013**, *5* (2), 588-593. DOI: 10.1002/cctc.201200420.

(26) Mattey, A. P.; Ford, G. J.; Citoler, J.; Baldwin, C.; Marshall, J. R.; Palmer, R. B.; Thompson, M.; Turner, N. J.; Cosgrove, S. C.; Flitsch, S. L. Development of Continuous Flow Systems to Access Secondary Amines through Previously Incompatible Biocatalytic Cascades. *Angew. Chem. Int. Ed. Engl.* **2021**, *60* (34), 18660-18665. DOI: 10.1002/anie.202103805.

(27) Koszelewski, D.; Müller, N.; Schrittwieser, J. H.; Faber, K.; Kroutil, W. Immobilization of Ω-Transaminases by Encapsulation in a Sol–Gel/Celite Matrix. *J. Mol. Catal. B: Enzym.* **2010**, *63* (1-2), 39-44. DOI: 10.1016/j.molcatb.2009.12.001.

(28) Shin, J.-S.; Kim, B.-G.; Shin, D.-H. Kinetic Resolution of Chiral Amines Using Packed-Bed Reactor. *Enzyme Microb. Technol.* **2001**, *29* (4-5), 232-239. DOI: 10.1016/s0141-0229(01)00382-9.

(29) Truppo, M. D.; Strotman, H.; Hughes, G. Development of an Immobilized Transaminase Capable of Operating in Organic Solvent. *ChemCatChem* **2012**, *4* (8), 1071-1074. DOI: 10.1002/cctc.201200228.

(30) Truppo, M. D.; Journet, M.; Strotman, H.; McMullen, J. P.; Grosser, S. T. Wpto Us9523107b2, Immobilized Transaminases and Process for Making and Using Immobilized Transaminase. 2014.

(31) The resin contains ~65 w/w% water.

(32) The immobilization was performed using enzyme loading exceeding the resin capacity. For assessing catalytic efficiency, we list the wt% corresponding to the amount of protein immobilized to the resin and present in the reaction.

(33) Guan, L. J.; Ohtsuka, J.; Okai, M.; Miyakawa, T.; Mase, T.; Zhi, Y.; Hou, F.; Ito, N.; Iwasaki, A.; Yasohara, Y.; et al. A New Target Region for Changing the Substrate Specificity of Amine Transaminases. *Sci. Rep.* **2015**, *5*, 10753. DOI: 10.1038/srep10753.

(34) John, R. A. Pyridoxal Phosphate-Dependent Enzymes. *Biochim. Biophys. Acta* **1995**, *1248* (2), 81-96. DOI: 10.1016/0167-4838(95)00025-p.

(35) Fitzpatrick, P. A.; Klibanov, A. M. How Can the Solvent Affect Enzyme Enantioselectivity? *J. Am. Chem. Soc.* **1991**, *113* (8), 3166-3171. DOI: 10.1021/ja00008a054.